13th ewtec 2019 Proceedings of the 13th European Wave and Tidal Energy Conference 1-6 Sept 2019, Naples, Italy

Tide-to-wire model development for realistic tide environments

Marios C. Sousounis, Joseph P. Tomy, Stéphane Paboeuf and Jonathan K. H. Shek

Abstract—**This paper presents the development of a tide-to-wire model with realistic tidal current environment under RealTide project which can be used as an open-source tool. Even though the free stream velocity of the tidal current can be predicted, the actual inflow at the turbine in a realistic environment is dynamically varying with time as well as the depth of the ocean. Local flow acceleration and enhanced lift due to dynamic stall effects may create unanticipated high structural loads on the turbine blades, which could cause structural damage and might also be important for fatigue considerations. The variation of power output in time is also a primary concern for grid compliance. To include both mechanical and electrical effects, a numerical model based on Blade Element Momentum Theory in Python is developed for prediction of the forces, torque and power output of the tidal turbine. The output torque of the Blade Element Momentum Theory is used as input to an electrical model developed in OpenModelica. The electrical model has an electrical generator which is actively controlled in order to perform maximum power point tracking and maximise the power capture from the tides. The rotational speed of the generator is fed back to the Blade Element Momentum Theory code in order to calculate the tip speed ratio. The final part of the paper focuses on validating the complete model with experimental results from the Sabella D10 tidal current turbine.**

Keywords—**Tidal energy; Electro-mechanical modelling; Blade element momentum; Permanent magnet generator; Maximum power point tracking.**

I. Introduction

TIDAL current turbines can supply Europe with clean, renewable and predictable energy. Including the predictable tidal current energy in the energy mix of Europe will reduce uncertainty of supply and help on providing a sustainable energy system for the future. The RealTide project aims to identify main failure causes of tidal turbines and to adapt key components to the complex tidal current conditions. Tidal currents move slowly compared to wind but possess larger energy density which results on large forces on the tidal turbines. Despite the large forces tidal turbines need to operate reliably under harsh conditions. Advances in the measurement of flow in highly energetic tidal currents allows the effects of both turbulence and ocean waves to be characterised. High resolution tidal current measurements can greatly improve the realistic modelling of a tidal current turbine. Through accurate modelling the understanding of the causes of failure in blades, seals, bearings, PTO & other critical components can be improved, de-risking financial investment by applying corrective measures. A step to this process is the development of models that can capture the physical phenomena that take place during a tidal current turbine operation.

The aim of this paper is to present a full realistic resource-to-grid dynamic model of a single tidal current turbine developed by Open Source software which can be used as a user-friendly tool. In order to do so three main parts of the tidal current conversion system have been identified: velocimetry, high accuracy tidal turbine modelling and electrical design for grid connection with the associated control structures. Section I.A. introduces the background information for tidal turbine modelling using Blade Element Momentum Theory (BEMT) and Section I.B. the main literature for resource-to-grid modelling of tidal current systems. Section II introduces the improvements to BEMT implemented. Section III explains the architecture of the user-friendly tool and validates the BEMT method developed in Python under different cases. Section IV presents the electrical system modelling and control in OpenModelica as a standalone model. The electrical model of Section IV and the BEMT turbine model of Section III are coupled through the process discussed in Section V. Results of the full resource-to-grid model are presented in Section VI. Conclusions are drawn in Section VII.

Paper ID: 1798. EWTEC 2019 conference track: Tidal Device Development and Testing. This work was supported by the European Union's Horizon 2020 research and innovation programme under grant agreement No 727689.

M. C. Sousounis is with the School of Engineering, Institute for Energy Systems, University of Edinburgh, Faraday Building, King's Buildings, Colin Maclaurin Road, Edinburgh, EH9 3DW, UK (e-mail: M.Sousounis@ed.ac.uk).

J.P. Tomy is Research Engineer at the Composite Materials Section within Expertise Department of Bureau Veritas Marine & Offshore Division, 8 Boulevard Albert Einstein, Nantes, France (e-mail: josephpraful@gmail.com).

S. Paboeuf is Head of Composite Materials Section within Expertise Department of Bureau Veritas Marine & Offshore Division, 8 Boulevard Albert Einstein, Nantes, France (e-mail: stephane.paboeuf@bureauveritas.com).

J. K. H. Shek is with the School of Engineering, Institute for Energy Systems, University of Edinburgh, Faraday Building, King's Buildings, Colin Maclaurin Road, Edinburgh, EH9 3DW, UK (e-mail: j.shek@ed.ac.uk).

A. *Tidal turbine modelling using Blade Element Momentum Theory*

A preliminary understanding of the development of the Blade Element Momentum theory is obtained from [1]. This document explains the derivation of the BEMT from momentum conservation equations. The BEMT is essentially a combination of two theories – the actuator disk momentum theory and the blade element theory.

The actuator disk momentum theory explains the power extracted by an actuator disk within a flow field. It is based on the Newton's second law, which equates the force experienced by the actuator disk as the rate of change of momentum of the fluid while passing through the disk. Based on the conservation of linear momentum and angular momentum, the induced velocities in the axial and tangential directions of the disk can be determined. However, the simplification of a multi-bladed rotor to a disk seems too general.

In the blade element theory, the blades are divided into different segments, known as blade elements. Each blade element is assumed to act independent of the other, so that the total force on the blade can be obtained by an integration of the forces on each individual blade element. The dynamic force on each blade element can be computed based on the local flow conditions at each blade element. The two key assumptions of the blade element theory are that there are no dynamic interactions between the blade elements and that the forces on the blade elements are solely determined by the lift and drag components.

BEMT combines both these theories to provide a theoretical formulation for the working of rotating blades within a fluid flow environment. The blade is divided into different blade elements, and each of these elements traces out annular regions as shown in Fig. 1. These annular regions are considered as individual annular disks and the axial momentum theory is applied on them to obtain the individual forces acting on them. Thereafter, the blade element forces are integrated to compute the total force acting on the blade and the power generated by the rotor. A detailed and well-explained derivation of the BEMT equations can be found in the work by Grant Ingram [1].

Referring to Fig. 1. if V1 and V2 represent the velocities at locations 1 and 2 respectively, then the axial induction factor, α is defined as $a = \frac{V_1 - V_2}{V_1}$. Similarly, if the blades rotate with an angular velocity of Ω and the blade element wake rotates at an angular velocity ω, then the tangential induction factor, b is defined as $b = \frac{\omega}{2\Omega}$.

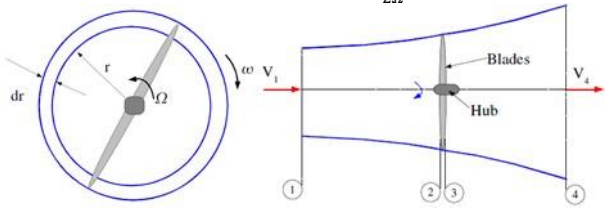

Fig. 1. Annular region traced out by a blade element (left) and axial stream around a wind turbine.

The application of conservation of linear momentum and angular momentum theories provides equations for the elementary thrust (dT) and the elementary torque (dQ) produced by the blade element in terms of these induction factors. These equations for dT and dQ are:

$$dT = \frac{1}{2}\rho V_1^2[4a(1-a)]2\pi r.dr \quad (1)$$

$$dQ = 4b(1-a)\rho V_1 \Omega r^3 \pi.dr \quad (2)$$

Here, ρ represents the density of the medium and r represents the radial position of the blade element from the hub centre. These elemental components can be then integrated for all the different blade elements to compute the total thrust and torque generated by the blade.

The elementary thrust and torque for a blade element can only be obtained by knowing the induction factors a and b. Each of these blade elements is an aerofoil section, and hence the forces on them can be expressed in terms of their lift and drag coefficients. This is one of the main assumptions of the BEMT, and by applying this, the elementary thrust and torque equations above (1) & (2) can be equated in terms of the lift (L) and drag (D) of the aerofoil section (Fig. 2). Solving these equations algebraically, we get the induction factors in terms of the lift and drag coefficients (C_L and C_D), as shown in (3) & (4).

$$\frac{a}{1-a} = \frac{\sigma[C_L \cos\varphi + C_D \sin\varphi]}{4\sin^2\varphi} \quad (3)$$

$$\frac{b}{1+b} = \frac{\sigma[C_L \sin\varphi - C_D \cos\varphi]}{4\sin\varphi\cos\varphi} \quad (4)$$

Where σ is defined as the local solidity ratio ($\sigma = \frac{Bc}{2\pi r}$, B = No of blades, c = chord length, r = radial location of blade element).

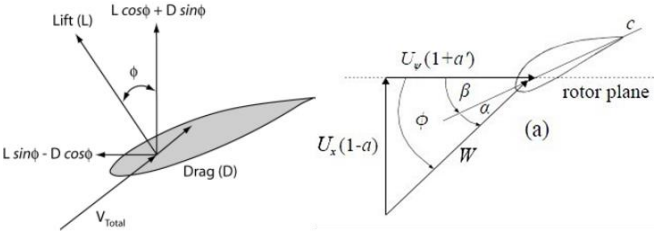

Fig. 2. Blade section diagrams showing force components (left) and velocity components (right).

The equations represented as (3) & (4) are known as the BEMT equations. The parameter σ, C_L and C_D are related to the position of the blade element, and its geometry. The local inflow angle φ is related geometrically to the inflow velocities and the induction factors, as can be seen in Fig. 2. Therefore, the BEMT equations can be solved for a given inflow condition and given blade geometry by obtaining suitable values for the induction factors a and b. The conventional method to obtain this solution is by following an iterative approach to converge on the solution for the induction factors at each blade element.

B. Tide-to-wire models

The literature regarding electrical modelling and control of Tidal Current Conversion System (TCCS) is limited especially if it is compared to research in offshore and onshore wind energy systems. An overview of the electrical design in TCCS and wave energy systems is presented in [2]. Authors present an overview of the electrical design options for ocean energy converters in general and in addition show the use of power electronics for generator control and grid connection. The simplification of [2] is that the resource-to-grid modelling presented is based on mathematical formulations and ideal operation of the control loops.

A comprehensive way of modelling dynamic resource-to-grid TCCSs is presented in [3] using physical components. The author develops dynamic electromechanical models of tidal current devices in detail, from resource to the grid connection, using mathematical linear and non-linear programming in MATLAB/Simulink. The results presented in [3] are compared against data provided by Andritz Hydro Hammerfest. The study also expands to modelling a number of electrical architectures for tidal current arrays.

Apart from studies that look at electrical and control modelling for tidal current devices as a complete system a number of researchers focus on specific aspects. Researchers in [4] compare pitch and stall regulated tidal current turbines during variable speed operation. Researchers in [5] use long sub-sea cables between the generator and the voltage-source converter (VSC) in order to transmit power to the grid. Comparing the types of generators in tidal current applications is performed in two separate studies under different conditions [6], [7]. In [6] authors compare all the types of generators that can be used in a tidal current system and summarise the advantages and disadvantages of each generator technology. In [7] researchers compare the Squirrel Cage Induction Generator (SCIG) and the Permanent Magnet Synchronous Generator (PMSG) in a tidal system with direct connection to shore using onshore power converters.

II. Blade Element Momentum Theory Improvements

C. Tip Losses

The BEMT does not consider the effects of vortex shedding from the tip of the blades and its root. Tip vortex shedding is a typical characteristic of fast-moving field rotors such as ship propellers and turbine blades. Since only the transfer of momentum from the flow field to the blade rotation is considered within the limits of the theory, the losses due to tip vortex shedding is not included in the theory. However, these losses are significant and need to be accounted for.

Most of the improved BEMT numerical models account for the tip losses by means of Prandtl correction factor. This is the same that is implemented in AeroDyn, wherein it is explained that "the Prandtl model simplifies the wake of a turbine by modelling the helical vortex wake pattern as vortex sheets that are convected by the mean flow and have no direct effect on the wake itself" [8]. The theory is characterized by introducing an additional correction factor for the induced velocity field, F which is given as:

$F = \frac{2}{\pi} cos^{-1} e^{-f}$ where $f = \frac{B}{2} * \frac{R-r}{r\,sin\varphi}$

B = Number of blades

R = Blade radius (in m)

r = Radial location of the blade element (in m)

φ = Inflow angle (in radians)

D. Hub Losses

The hub loss correction factor is an improvement that considers the effect of the vortices that are shed at the blade-hub connection. The nature of the hub loss correction factor is the same as that of the tip loss correction factor, but with a sharp decrease towards the root of the blade. The equation for the hub loss correction would have the factor as $f = \frac{B}{2} * \frac{r-R_{hub}}{r\,sin\varphi}$

E. High Induction Factor

The induction factor is defined as a ratio of change in velocity of flow between the free stream velocity and the velocity at the blade. The theoretical limit of the axial induction factor, α in BEMT is in the range of 0 to 0.5. Since $V_2 = V_1(1-a)$ and $V_4 = V_1(1-2a)$, at induction factors above 0.5, the BEMT would predict a negative wake velocity at the turbine blades. This represents the theoretical limit of the BEMT, whereas in reality this would mean that the wake has become turbulent.

While developing the BEMT algorithm, existing literature was referred to identify suitable formulations to account for this correction. Accordingly, the Glauert correction and the quadratic correction used in *TidalBladed* were found to be the most suitable and easily implementable empirical formulations.

F. Root finding algorithms

The iterative approach followed to find the solution to the induction factors may be computationally intensive when it comes to depth-wise and time-varying input velocity fields that simulate realistic flow conditions. Moreover, these computations need to be done for each blade element, at each instant of time. Andrew Ning [9] suggests an alternative approach for optimization by parameterization of the BEM equations by one variable, i.e. the local inflow angle. This avoids the need for a two-variable optimization, and one-variable root finding algorithms can be used to determine an optimum solution. This method has been implemented in the Matlab code developed by University of Edinburgh, which is referred in [10].

The advantage of having single-variable equations is that faster optimization algorithms can be employed. One such optimization algorithm mentioned in the work by

Ning [9] is the Brent's root-finding algorithm. Within the Python code, such a single variable optimisation is employed to enhance the speed of computations.

G. Dynamic Stall

The variation of fluid velocity over the rotor disk creates unsteady angles of attack at the blade sections. These cause dynamic stall events and need to be accounted for by a dynamic stall model.

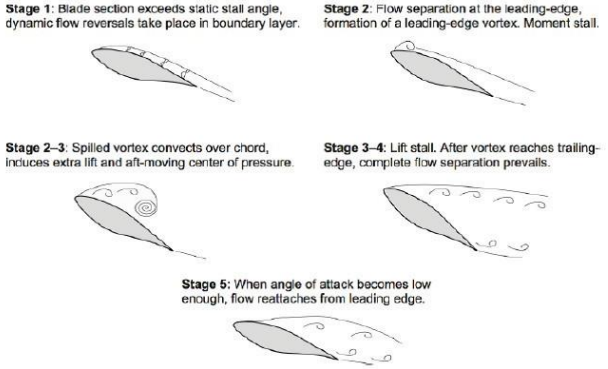

Fig. 3. Conventional stages of Dynamic Stall [11].

The conventional stages of dynamic stall are represented in Fig. 3. Of principal importance is the increased lift generated by the convecting vortex, which can generate unexpectedly high forces and rotational speeds for the tidal turbine. The Beddoes-Leishman model is used as the basis for development of many of the actively used dynamic stall modules today. The basic Beddoes-Leishman model is explained by Leishman in [11]. A modified Beddoes-Leishman model, as implemented in the University of Edinburgh BEMT code, has been proposed in [12].

H. Wake Models

The steady inflow assumption of the BEMT is not a realistic assumption for industrial flows. In reality, the inflow is time variant and the dynamic wake of the inflow needs to be incorporated in the BEMT model. BEMT is developed based on the assumption that the wake reacts instantaneously to the changes in blade loading. This means that the solution for a and b using the BEMT equations needs to be obtained for each time step of the dynamic simulation. This is referred to as an equilibrium wake model, and is computationally intensive [13].

In reality, the equilibrium wake model does not take into account the time lag for the dynamic effects to take place. The changes in blade loading change the vorticity that is trailed into the rotor wake and these effects take a finite time to change the induced flow field. Consideration of this time lag effect is called as a dynamic wake approach.

I. Rotational Augmentation

Rotational augmentation considers the effect of the rotation of the blades on flow acceleration. The rotation of the blades induces a centrifugal force which causes a span-wise flow, and a Coriolis force which accelerates the flow towards the trailing edge. These effects reduce the adverse pressure gradient to promote flow reattachment and delay the separation. This in turn leads to an augmentation of lift from the stationary value [10]. The Lindenburg model for rotational augmentation is implemented as an option within the code, following the calculation procedure mentioned in [10].

III. Blade Element Momentum Tool

J. Program Architecture

BEMT predicts the performance for a single blade element rotating as an annular disc. Extending this theory to a full tidal turbine working in a dynamic environment involves numerical computations over multiple iterative parameters. Only considering the geometry of the turbine, this would be in the form of integrating the results for a single blade, and then for multiple blades. Further, multiple operating conditions present themselves as iterative parameters in the form of time steps of computations and varying inflow velocities.

These iterative parameters interact with each other over the computational procedure. For example, the inflow velocity at a blade element which is required for BEMT computations, requires the knowledge of its instantaneous position. This instantaneous position depends on the rotational speed, and the blade under consideration. Such interactions between the loop variables would mean that the program architecture needs to be suitably designed to avoid for any undesirable computational complexities.

The various iterative loops inherent to the computational framework have been identified and represented as a flowchart in Fig. 4. From an intuitive approach starting from the most elemental application of BEMT, the theory is applied to each blade element. This corresponds to the basic level of computations and hence the innermost loop. Subsequently the computations are extended to each blade, for each time step and then for each operating condition. These are evident from the loop structure in Fig. 4. Also included in this flowchart is the manner in which the electrical module is integrated within the BEMT calculations.

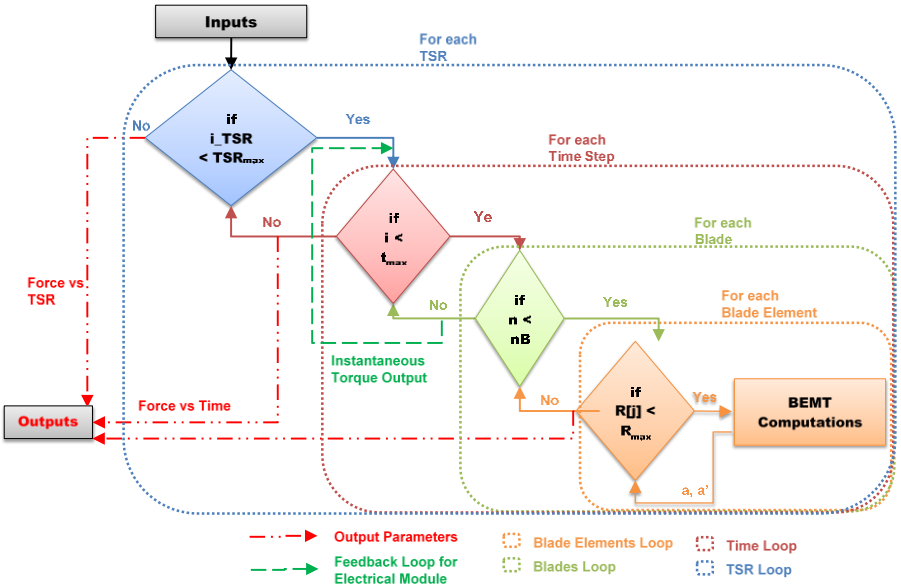

Fig. 4. Program architecture flowchart.

K. *User Interface*

Although the software developed is not comprehensively designed for commercial use, the presence of a user interface enhances the usability of the code. The prime focus of the work is the development of a functional tool; but a considerable sight has also been given into the development of a user-friendly interface. The code is expected to be used in the future by users who are not familiar with Python hence it is advisable to disseminate only the relevant information to the user.

Giving due consideration to all these factors, a simple user-interface was developed using the Python Tkinter library. A snapshot of this is shown in Fig. 5.

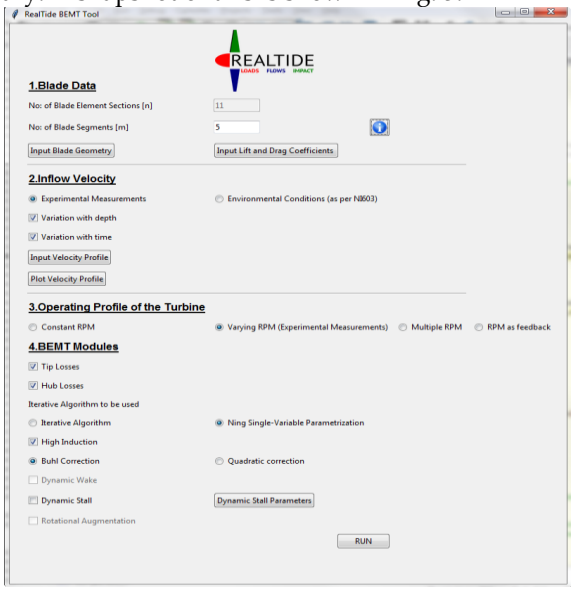

Fig. 5. Graphical User Interface for the Python code.

During the design of the user interface, various user input variables and possible scenarios of usage of the tool were analysed. Subsequently, the following parameters were identified as critical user input values - Geometry of the tidal turbine, input velocity profile, operating conditions of the tidal turbine and various BEMT improvements that need to be considered in the analysis.

L. *Velocity Profile*

Perhaps the most important input velocity parameter is the velocity profile of the inflow. Simulating a real-world scenario would require the program to consider the variation of the velocity profile in position as well as time. However, as a simplification of this case, the real-world scenario of 3-dimensional time varying flow, is simplified into a 2-dimensional time varying flow at the rotor disk. This would mean that only the x-component of the velocity (U_{axial}) is considered, and this is taken varying depthwise (z-direction) as well as in time. Therefore, $U_{axial} = f(z,t)$.

The simplest means of accepting such a velocity profile is to ask the user to input a matrix of velocity values that vary in z and t. However, the program needs to be adapted to practical scenarios of availability of such values. Such practical considerations are taken in accordance with usual experimental procedures.

Fig. 6 shows a typical experimental set-up. Sensors are placed on the blades of the turbine to measure the strain on them and the rotor thrust. Also, the measurement of the rotor torque is done by sensors on the nacelle. The velocity measurements are taken using a flow velocity sensor, placed at a distance D in the downstream direction of the flow. This velocity sensor could be an Acoustic Doppler Current Profiler (ADCP), which generates sound waves to the bottom of the surface and characterises the velocity at different points based on the Doppler shift of the returning waves [14].

The usual procedure is to obtain the velocity (V_{ref}) at the sensor location (z_{ref}) and then extrapolate it to the depth of the tank using a power law. The power law depends on the depth of the tank, and it assumes zero velocity at the bottom of the basin (no slip boundary condition), with a power variation for increasing z. The corresponding

velocity (V) at any point (z) is given in terms of a power factor (pf) as $V = V_{ref} * \left(\frac{z}{z_{ref}}\right)^{pf}$.

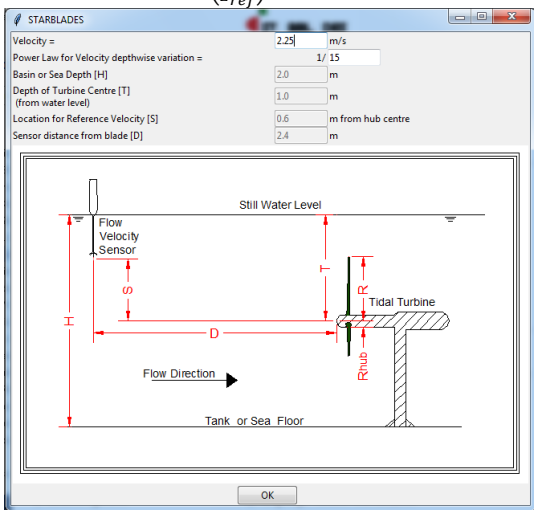

Fig. 6. User input of velocity parameters (constant velocity).

Now, the input from the user would be the reference velocity, V_{ref}. This can be a constant value (in case of steady flow) or a time varying flow. In case the depth-wise variation is to be considered, the user also provides the power factor, and the code extrapolates the velocity data along the depth. For a constant velocity input, the input window that appears is as shown in Fig. 6. In the case that the velocity input is time varying, then the user needs to specify a file, which includes V_{ref} as a function of time.

M. Rotation Speed

The rpm input can be accepted from the user in four different ways. These possible rpm input types are: constant rpm, time-varying rpm measurements from experimental data, multiple rpm for multiple operating conditions, and rpm as feedback from the electrical module. But in all of these cases, for a given operating condition and given time step, i.e. inside the TSR loop and time loop, the rpm value is a constant. The only difference is how this constant rpm value is computed outside the blade loop.

For a constant rpm input, the rpm variable retains the constant value throughout the computation. In the case of multiple TSRs, the rpm variable takes its value inside the TSR loop, corresponding to the current TSR step. In case of experimental measurements, the rpm variable takes its value inside the time loop, corresponding to the current time step. Implementation of rpm value as feedback is described in Section V.

N. Solver

Within the Python code, the computations involving BEMT are coded in the form of various functions and scripts. BEMT computations are performed considering each blade element as an annular disc, rotating around the hub, absorbing energy from the incoming flow. The elementary BEMT equations are developed considering a constant inflow velocity into the turbine. This consideration enables one to compute the elementary forces on the blade elements on one blade and extend it to all the other blades. However, while simulating a realistic environment, the inflow has a depth-wise varying profile.

A stepwise simplification of the BEMT computations is mentioned below. More details can be accessed from [15]. These computations are performed at each blade element of each blade.

Step 1: Instantaneous rotation speed of the turbine
Step 2: Instantaneous position of the blade element
Step 3: Axial velocity at the blade element
Step 4: Angular velocity and local speed ratio
Step 5: Initial values of φ, a and b
Step 6: Iterative solution for a and b

O. Validation

The validation of the BEMT computations have been made with available experimental and CFD results. Being a relatively new industry, there are not many test cases available within the tidal turbine industry, especially for the dynamic analysis. However, the application of BEMT is the same in the case of wind turbines as well. The fluid mechanics of the operating scenario is the same, with the change only in the fluid environment. Moreover, the amount of experimental research conducted in the aerodynamic industry, particularly for wind turbines, is much more. Many of the commercial tidal turbine codes have also used wind turbine data for validation. Hence, the use of such data is also considered for the validation process.

The sequence for validation studies performed is in the following order. Initially, the code is checked for accuracy in a static analysis case. Thereafter, the dynamic stall module is validated with experimental results of aerofoils available from NREL [16]. Subsequently, the code needs to be checked for a dynamic analysis of a tidal turbine in tank testing facilities. This includes time-varying force and velocity measurements. Ultimately, the tool will be validated with real-sea condition measurements. The first two steps of this validation process has been completed, and some of the results are graphically represented in Fig. 7 to Fig. 10.

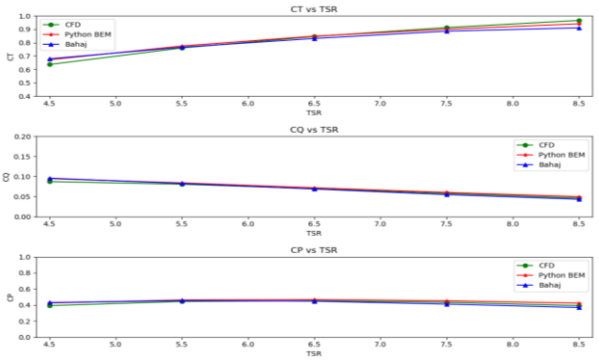

Fig. 7. Comparison of CT, CQ, and CP - Bahaj validation.

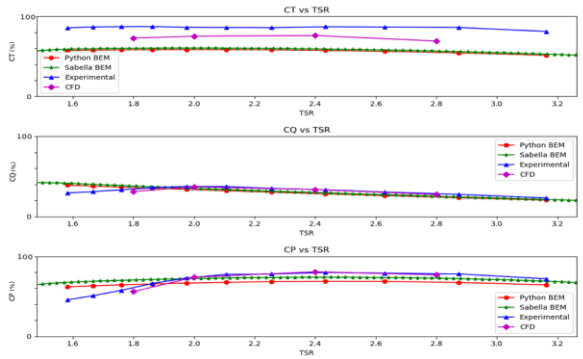

Fig. 8. Sabella D10 validation case.

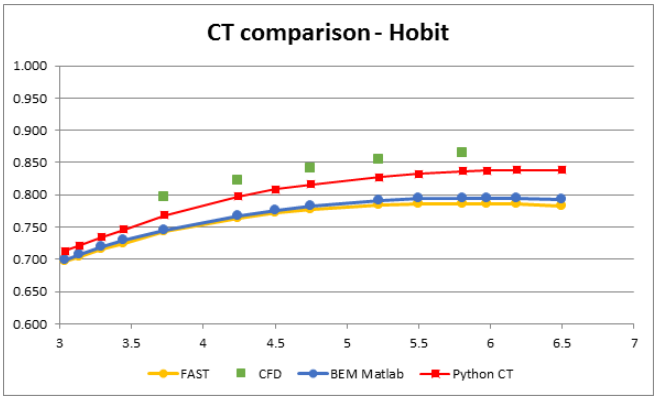

Fig. 9. Comparison of CT - HOBIT validation.

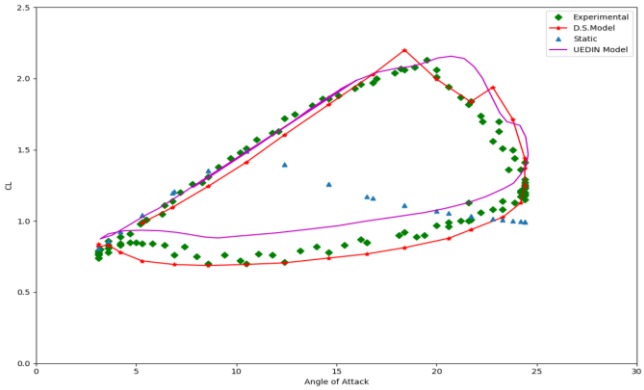

Fig. 10. Dynamic Stall validation – NREL S814.

The blade geometry and operating conditions used are not included here for the sake of brevity. They can be referred from [15]. The validation studies show reasonably accurate estimation of the thrust, torque and power coefficients in line with the benchmark results. The final two stages of validation are in progress.

IV. Electrical Modelling and Control of Tidal Current System

The block diagram of the electrical part of the tidal current system developed in OpenModelica is depicted in Fig. 11. The electrical system configuration is based on the Sabella D10 tidal current turbine and can be found in [17].

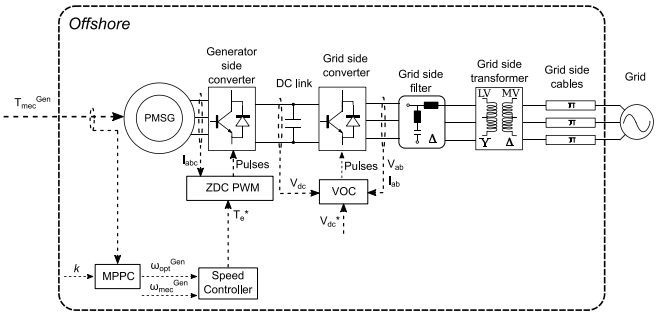

Fig. 11. Block diagram of the electrical model of the tidal system developed in OpenModelica.

The input to the electrical model is the mechanical torque T_{mec}^{Gen} which is the output from the tidal current turbine model discussed in Sections II and III. The electrical model also includes a maximum power point tracking (MPPT) control strategy with the use of a speed controller and a zero d-axis current controller, the Voltage Oriented Controller to export the generated power at fixed frequency and the grid side power transmission system. All the above modelling aspects are expanded on the following sections.

P. The electrical generator

The electrical generator of the Sabella D10 is a direct drive (DD) PMSG and therefore there is no gearbox between the generator and the turbine. Table I shows some of the specifications used to model the electrical generator in OpenModelica.

TABLE I
PERMANENT MAGNET SYNCHRONOUS GENERATOR SPECIFICATIONS

Symbol	Quantity	Value	Unit
P_{gen}^{R}	Rated power	500	kW
P_{gen}^{M}	Maximum Power	1000	kW
T_e^R	Rated electromechanical torque	490000	Nm
pp	Pole pairs	120	–
w_{mec}	Mechanical rotational speed range	0 – 2.09	rad/s

The DD PMSG is controlled from the zero d-axis controller (ZDC) which aims to set the electromechanical torque of the generator T_e equal to the desired electromechanical torque T_e*.

Q. The generator zero d-axis controller (ZDC)

The zero d-axis current controller for PMSG is described in [18] for wind energy systems and in [7] for a tidal system. The aim of the ZDC controller is to control the active power of the generator by controlling the generator T_e which has a linear relationship with the q-axis current component of the stator, i_{qs}. The block diagram of the ZDC controller can be seen in Fig. 12.

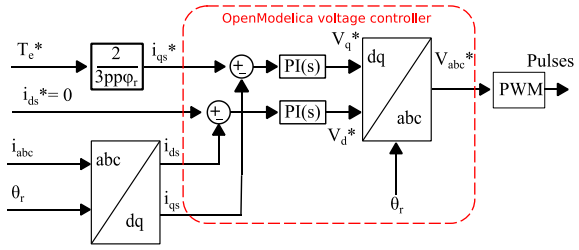

Fig. 12. Block diagram of the ZDC controller developed in OpenModelica.

For the successful operation of the ZDC controller the reference electromagnetic torque T_e^* is required as input. The appropriate value of the T_e^* is determined by the speed controller and is discussed in Section R. In addition, the three phase current i_{abc} at the output of the generator and the rotational angle of the generator rotor θ_r are required as inputs.

R. *Maximum power point tracking*

The aim of the MPPT system is to control the tidal turbine's tip speed ratio in order to achieve the highest possible hydrodynamic coefficient. In order to achieve the MPPT first the operating points where maximum Cp is achieved must be identified. The operating points at which the Cp is maximised for all the tidal current velocities form the maximum power point curve (MPPC). The MPPC is calculated using equation (5) by simulating the BEMT turbine for a number tidal current velocities and the range of turbine speeds given in Table I.

$$P_{mec} = k^2 \cdot \omega_{opt}^{Gen\,3} \Leftrightarrow \omega_{opt}^{Gen} = \sqrt[3]{\frac{P_{mec}}{k^2}} \tag{5}$$

The speed controller is responsible of comparing the optimum generator speed, ω_{opt}^{Gen} and the measured generator speed, ω_{mec}^{Gen} and produce the reference electromagnetic torque signal, T_e^*, to be used as input to the ZDC controller.

S. *Grid side modelling and control*

The power generated by the electrical generator is delivered to the grid through the "Grid side converter" as shown in Fig. 11. The "Grid side converter" is controlled by the Voltage Oriented Controller (VOC) with decoupled controllers which ensured constant DC link voltage, constant frequency output synchronised with the grid voltage for the AC side and control over the amount of reactive power flow depending on the grid requirements. The fundamentals of the VOC are discussed in [19]. The grid side cables for power transmission are modelled as a network of π-sections. The length of the cables is assumed to be 2km since this is the distance between the deployed Sabella D10 tidal turbine and the southeast coast of Ushant [17].

V. Coupling Process of BEMT Turbine and Electrical Model

The coupling process involves converting the Modelica model (.mo file) to a Functional Mock-up Unit (FMU) and managing the electrical model inputs and outputs from Python. Managing the FMU from python requires a Python library that can control FMUs such as pyFMI or FMPy. Fig. 13 shows the process to convert the Modelica electrical model to an FMU. More details about the FMU can be found in [20].

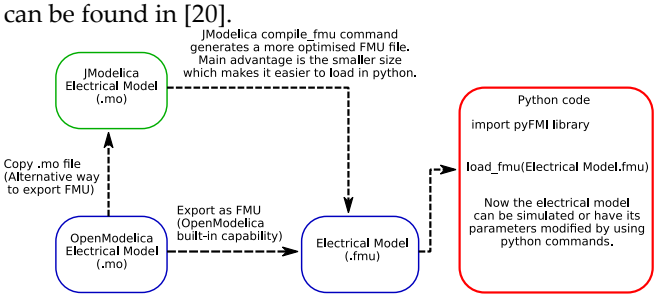

Fig. 13. Process to generate the FMU of the electrical model developed in OpenModelica and load it in python.

After generating the FMU file the BEMT Python code and the FMU loaded in Python need to exchange information at regular intervals. This is because the turbine operation is affected by the generator speed and the generator speed is affected by the mechanical torque input to the generator shaft. Therefore it is of crucial importance that the exchange of information between the BEMT code and the FMU, which contains the electrical model, is at regular intervals in order to capture the realistic operation. This is achieved by having both, the BEMT code and the FMU, in a while time loop which advances at this regular time step. An overview of this process is depicted in Fig. 14.

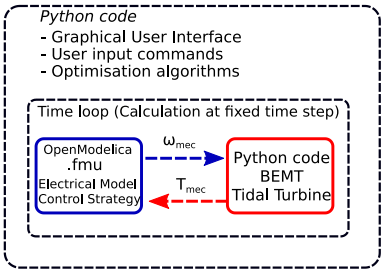

Fig. 14. Coupling of BEMT code and FMU. Exchange of information at regular intervals.

Following the processes described in Fig. 13 and Fig. 14 the coupled BEMT and electrical model can be simulated to generate realistic results.

VI. Tide-to-Wire Results of Coupled Model

The coupled electrical and BEMT model of the tidal current conversion system is simulated under realistic flow. The block diagram of the full system is depicted in Fig. 15 and the results are presented in Fig. 16.

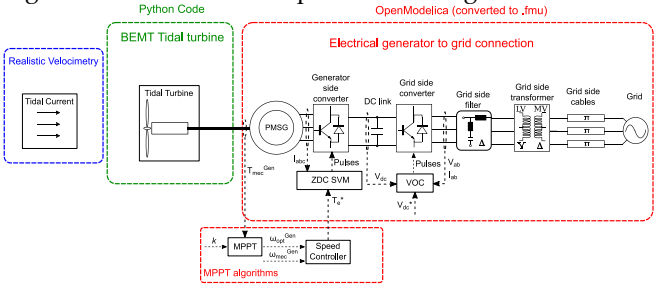

Fig. 15. Block diagram of the complete resource-to-grid system.

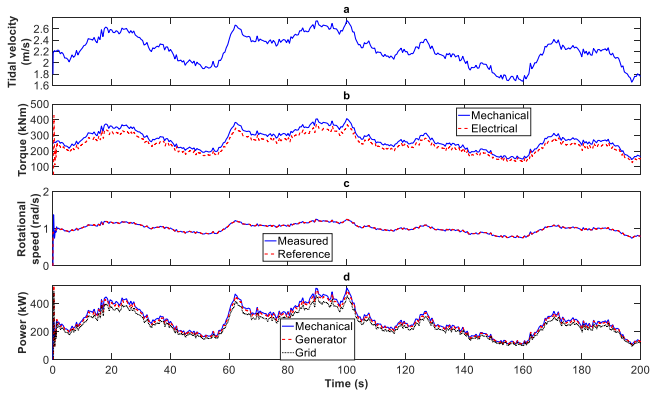

Fig. 16. Coupled system simulation (a) Tidal current velocity input at hub height. (b) Mechanical and electrical torque. (c) Reference and measured rotational speed. (d) Averaged mechanical, generator and grid power.

The coupled simulation results presented in Fig. 16 depict a number of variables that can be exported from resource-to-grid tool presented in this paper. The tidal current velocity used as input to the model was acquired from high resolution measured data at EMEC. In Fig. 16c it is shown that he generator is accurately controlled to follow the reference velocity achieving peak power capture from the tides. The mechanical power captured is efficiently exported to the grid and using this tool grid connection and power transfer can be studied further.

VII. Conclusion

In this paper a realistic resource-to-grid model of a tidal current conversion system is described. The model is presented as a novel software tool which combines realistic tidal current input, high accuracy calculations of the forces acting on the blades using BEMT and connection to a generic electrical model with all the associated control structures as well as grid connection. In addition, all the software packages used are Open Source which makes it widely accessible and open to changes. Based on the results presented, the BEMT developed in Python is showing a good match with experimental results. The integration of the electrical model with the Python-based BEMT tidal turbine is also explained. This tool can be used as a starting point in order to study what causes failures in tidal turbines and develop ways of monitoring or reducing them through control or structural design. In future research a CFD tidal turbine model will be developed in order to couple it to the electrical model and validate the tool further.

Acknowledgement

The authors would like to thank Nicolas Erwann and Julie Marcille from Sabella for their help and support in producing this paper. Field measurements from the EMEC tidal test site were acquired under the ReDAPT project (2010-2015) which was co-funded by the Energy Technologies Institute (ETI), UK.

References

[1] G. Ingram, "Wind Turbine Blade Analysis using the Blade Element Momentum Method. Version 1.1," Durham, 2011.

[2] R. Alcorn and D. O'Sullivan, *Electrical Design for Ocean Wave and Tidal Energy Systems*. The Institution of Engineering and Technology, 2014.

[3] M. C. Sousounis, "Electro-Mechanical Modelling of Tidal Arrays," The University of Edinburgh, 2018.

[4] B. Whitby and C. E. Ugalde-Loo, "Performance of Pitch and Stall Regulated Tidal Stream Turbines," *IEEE Trans. Sustain. Energy*, vol. 5, no. 1, pp. 64–72, Jan. 2014.

[5] M. C. Sousounis, J. K. H. Shek, and M. A. Mueller, "Modelling, control and frequency domain analysis of a tidal current conversion system with onshore converters," *IET Renew. Power Gener.*, vol. 10, no. 2, pp. 158–165, Feb. 2016.

[6] S. Benelghali, M. E. H. Benbouzid, and J. F. Charpentier, "Generator Systems for Marine Current Turbine Applications: A Comparative Study," *IEEE J. Ocean. Eng.*, vol. 37, no. 3, pp. 554–563, Jul. 2012.

[7] M. C. Sousounis, J. K. H. Shek, R. C. Crozier, and M. A. Mueller, "Comparison of Permanent Magnet Synchronous and Induction Generator for a Tidal Current Conversion System with Onshore Converters," in *Industrial Technology (ICIT), 2015 IEEE International Conference on*, 2015, pp. 2481–2486.

[8] P. J. Moriarty and A. C. Hansen, "AeroDyn Theory Manual," Golden, CO, Jan. 2005.

[9] S. Andrew Ning, "A simple solution method for the blade element momentum equations with guaranteed convergence," *Wind Energy*, vol. 17, pp. 1327–1345, Jul. 2014.

[10] G. T. Scarlett, B. Sellar, T. van den Bremer, and I. M. Viola, "UNSTEADY HYDRODYNAMICS OF A FULL-SCALE TIDAL TURBINE," in *6th European Conference on Computational Mechanics (ECCM 6)*, 2018, no. June.

[11] G. Leishman, *Principles of Helicopter Aerodynamics*, 1st ed. New York: Cambridge University Press, 2000.

[12] W. Sheng, R. A. M. Galbraith, and F. N. Coton, "A Modified Dynamic Stall Model for Low Mach Numbers," *J. Sol. Energy Eng.*, vol. 130, no. 3, p. 031013, 2008.

[13] DNV GL - Energy, "Tidal Bladed Theory Manual," Bristol, UK, 2014.

[14] B. Sellar and G. Wakelam, "Characterisation of Tidal Flows at the European Marine Energy Centre in the Absence of Ocean Waves," *Energies*, vol. 11, no. 1, p. 176, Jan. 2018.

[15] J. P. Tomy, "Blade Element Momentum Theory numerical model of a tidal turbine in a realistic time-dependent environment," Institut Catholique Arts et Metiers, 2019.

[16] J. M. Janiszewska, R. R. Ramsay, M. J. Hoffmann, and G. M. Gregorek, "Effects of grit roughness and pitch oscillations on the S814 airfoil," Golden, CO, Jul. 1996.

[17] S. Paboeuf, P. Yen Kai Sun, L.-M. Macadré, and G. Malgorn, "Power Performance Assessment of the Tidal Turbine Sabella D10 Following IEC62600-200," in *ASME 2016 35th International Conference on Ocean, Offshore and Arctic Engineering*, 2016, pp. 1–10.

[18] B. Wu, Y. Lang, N. Zargari, and S. Kouro, "Variable-Speed Wind Energy Systems With Synchronous Generators," in *Power Conversion and Control of Wind Energy Systems*, 1st ed., Hoboken, New Jersey: John Wiley & Sons, Inc., 2011, pp. 275–316.

[19] B. Wu, Y. Lang, N. Zargari, and S. Kouro, "Power Converters in Wind Energy Conversion Systems," in *Power Conversion and Control of Wind Energy Systems*, John Wiley & Sons, Inc., 2011, pp. 87–152.

[20] M. Association, "Functional Mock-up Interface," 2018. [Online]. Available: https://fmi-standard.org/. [Accessed: 26-Nov-2018].